Macromol. Symp. **2007**, 248, 82–93

DOI: 10.1002/masy.200750209

Scope for Accessing the Chain Length Dependence of the Termination Rate Coefficient for Disparate Length Radicals in Acrylate Free Radical Polymerization

Tara M. Lovestead, Thomas P. Davis, Martina H. Stenzel,
*Christopher Barner-Kowollik**

Summary: A method that utilizes reversible addition fragmentation chain transfer (RAFT) chemistry is evaluated on a theoretical basis to deduce the termination rate coefficient for disparate length radicals $k_t^{s,l}$ in acrylate free radical polymerization, where *s* and *l* represent the arbitrary yet disparate chain lengths from either a "short" or "long" RAFT distribution. The method is based on a previously developed method for elucidation of $k_t^{s,l}$ for the model monomer system styrene. The method was expanded to account for intramolecular chain transfer (i.e., the formation of mid-chain radicals via backbiting) and the free radical polymerization kinetic parameters of methyl acrylate. Simulations show that the method's predictive capability is sensitive to the polymerization rate's dependence on monomer concentration, i.e., the virtual monomer reaction order, which varies with the termination rate coefficient's value and chain length dependence. However, attaining the virtual monomer reaction order is a facile process and once known the method developed here that accounts for mid-chain radicals and virtual monomer reaction orders other than one seems robust enough to elucidate the chain length dependence of $k_t^{s,l}$ for the more complex acrylate free radical polymerization.

Keywords: backbiting; chain length dependent termination (CLDT); kinetics; reversible addition fragmentation chain transfer (RAFT); simulations

Introduction

Free radical polymerization (FRP) is a facile, cheap and often environmentally friendly process (i.e., one that can occur at room temperature and without solvent addition) that is used to synthesize materials for numerous applications, including adhesives, coatings, contact lenses and dental restorative materials.[1–4] In lieu of the many current applications, market needs continue to demand for more sophisticated materials for highly specific end-use applications. To this end, controlled/living FRP techniques are being developed to generate functional and complex molecular architectures, such as, block copolymers; core-shell nanoparticles; branched structures; and star and graft polymers.[5–13] However, the ability to design novel materials and control the polymerization depends on *a priori* knowledge of the FRP rate coefficients.

Of the three most important reaction steps that constitute FRP, i.e., initiation, propagation and termination, the termination process is the most complex. Much work has been carried out to characterize the termination rate coefficient (k_t) and how it depends on the polymerization

---

Centre for Advanced Macromolecular Design, School of Chemical Sciences and Engineering, The University of New South Wales, Sydney, New South Wales 2052, Australia
E-mail: camd@unsw.edu.au

conditions, e.g., the temperature; pressure; solvent concentration; reaction medium viscosity and the growing radical's size.[14–26] Previously, the dependence of the termination rate coefficient on the radical's size for equal size radicals, i.e., α, where $k_t^i \propto i^{-\alpha}$ and i represents the average radical size when only one reversible addition fragmentation chain transfer (RAFT) distribution exists, was ascertained utilizing RAFT chemistry.[19,25,27] This method termed the RAFT chain length dependent termination (RAFT–CLD–T) method extracts the termination rate coefficient as a function of chain length (k_t^i) from the on-line determination of the polymerization rate as a function of time, $R_p(t)$, and hence, allows for access to k_t's chain length dependency, i.e., the scaling exponent α when the chain length dependency follows a power law relationship.

The RAFT–CLD–T technique was exemplified on styrene[25,27] and later successfully mapped the chain length dependence of k_t for methyl acrylate (MA),[28] butyl acrylate,[29] dodecyl acrylate[30] and methyl methacrylate.[31] Additionally, the simultaneous dependence of k_t on radical size and monomer conversion was mapped using the RAFT–CLD–T methodology for MA[32] and vinyl acetate.[33] Another accurate and reliable method for accessing the chain length dependence of the termination rate coefficient (i.e., α, where $k_t^i \propto i^{-\alpha}$) is the non-stationary single pulse–pulsed laser polymerization–RAFT (SP–PLP–RAFT) technique.[23,34]

Recently, a method for deducing the chain length dependence of the termination rate coefficient for both similar and disparate size radicals, i.e., both α and φ, where $k_t^{s,l} \propto (sl)^{-\varphi/2}$, was introduced.[35] This method is based on the original RAFT–CLD–T method, which was modified for the parallel polymerization of two RAFT species of disparate average chain lengths, s and l. The method was exemplified theoretically using styrene because its kinetic rate coefficients and material properties are well known and its polymerization kinetics exhibit nominal chain transfer and other interfering side reactions. The previously published manuscript details a thorough theoretical assessment of the method and its ability to access k_t's chain length dependence for both similar and disparate size radicals (i.e., both α and φ) for slowly propagating monomers within reasonable accuracy regardless of the input kinetic parameters and/or the relationship assumed for the termination rate coefficient's chain length dependence.[35]

Acrylates are used extensively in industry and complete characterization of their FRP kinetics would be advantageous as is evident from the numerous investigations of acrylate kinetics found in the literature.[15,21–23,28–30,32,36–44] Testing the method – at least theoretically – to elucidate $k_t^{s,l}$ for fast propagating monomers such as acrylates is an interesting problem. For one, acrylates undergo side reactions such as inter- and intramolecular chain transfer (i.e., chain transfer to polymer and backbiting, respectively), and thus, whether or not these side reactions will impact the method's ability to elucidate the termination kinetic coefficient from only the polymerization rate data needs to be examined.[2,45–49] Additionally, the RAFT–CLD–T method relies on accurate on-line determination of the polymerization rate and – given their rapid polymerization – acrylates seem as an attractive option for experimental validation of this procedure. Thus, the impact of fast propagation, backbiting and mid-chain radical reactions on the method's ability to obtain accurately the chain length dependence of k_t for both similar and disparate size radicals is investigated with the goal of aiding the experimentalist in choosing the optimum polymerization system for validating the recently introduced $k_t^{s,l}$ methodology.

Model Development

The method presented here builds upon the basic FRP reactions and the reactions that constitute RAFT process, which have been detailed extensively in prior publications and will not be reiterated here.[9,50] The method is based on the direct measurement of the polymerization rate as a function of time, $R_p(t)$, which is given by equation 1.

$$R_p(t) = -\frac{d[M]}{dt} = k_p[M][P\cdot] \tag{1}$$

Here, t is the polymerization time, [M] is the monomer concentration, k_p is the propagation rate coefficient, and $[P^\cdot]$ is the propagating radical concentration. R_p relates to the termination rate coefficient, k_t, via the well-known classical equations for the initiation and termination rates and the change in the radical concentration with time to provide the following chain-length averaged k_t as a function of time, $\langle k_t \rangle(t)$.[30]

$$\langle k_t\rangle(t) = \frac{2fk_d[I]_0 e^{-k_d t} - \dfrac{d\left(\dfrac{R_p(t)}{k_p^*\left([M]_0 - \int_0^t R_p(t)dt\right)^{\omega}}\right)}{dt}}{2\left(\dfrac{R_p(t)}{k_p^*\left([M]_0 - \int_0^t R_p(t)dt\right)^{\omega}}\right)^2} \tag{2}$$

Here, k_d is the initiator decomposition rate, [I] is the initiator concentration and f is the initiator efficiency. Note that no assumption of a steady state radical concentration is made. Additionally, the non-classical relationship between R_p and the monomer concentration due to the formation of less reactive mid-chain radicals is accounted for using equation 3, which introduces a modified propagation rate coefficient, k_p^*, and the possibility of accounting for virtual monomer reaction orders, ω, other than one.[30]

$$k_p^* = k_p[M]_0^{1-\omega} \tag{3}$$

The unique attributes of the RAFT mediated FRP (i.e., a linear increase in the average radical length (i) and a nearly monodisperse radical chain length distribution ($i \approx j$) allows for the chain-length averaged k_t to be related directly to the microscopic $k_t^{i,i}$ at any point in time. Thus, the chain length dependence of the termination rate coefficient for equal size radicals, i.e., α (equation 4), is accessible when R_p, the molecular weight distribution (MWD) evolution and a value for the termination rate coefficient for two unimers ($k_t^{1,1}$) is assumed.

$$k_t^{i,i} = k_t^{1,1}(i \cdot i)^{-\alpha/2} \tag{4}$$

To elucidate the chain length dependence of the termination rate coefficient for disparate average size radicals, i.e., φ, where $k_t^{s,l} \propto (sl)^{-\varphi/2}$, two RAFT distributions are generated by simulating the reaction of a system comprised of monomer, initiator, RAFT agent and a macroRAFT species of initial chain length greater than one via implementing two complete RAFT mediated FRP reactions into the kinetic modeling program PREDICI®.[35,51] Chains from different distributions are denoted using the superscript s or l for the "short" or "long" chain species, respectively, for example, $[P_i^{s\cdot}]$ represents a radical concentration of arbitrary chain length i from the distribution of "short" chains s. Thus, initiation, propagation, and macroRAFT species generation as well as termination occur for each distribution. In addition, core equilibrium and termination occurs between either the l or s chain macroRAFT species and reactive radical, respectively. Note that within a given RAFT distribution the individual chain lengths are denoted i and j and are assumed to be approximately equivalent and chains belonging to different distributions are denoted s and l. Assuming that each RAFT distribution is adequately represented by its average chain length, the average termination rate coefficient is given by equation 5, i.e., the total termination rate divided by the square of the total radical concentration.[35]

$$\langle k_t\rangle = \frac{k_t^{s,s}[P_s\cdot]^2 + 2k_t^{s,l}[P_s\cdot][P_l\cdot] + k_t^{l,l}[P_l\cdot]^2}{([P_s\cdot] + [P_l\cdot])^2} \tag{5}$$

Here, $[P_s^{\cdot}]$ and $[P_l^{\cdot}]$ are the concentration of "short" and "long" radicals, respectively, and the total termination rate (the numerator) is equal to the sum of the termination rate for chains of approximately identical size (*ss* or *ll*) and disparate size (*sl* and *ls*). When equal concentrations of reacting species exist (i.e., $[P_s^{\cdot}] = [P_l^{\cdot}]$), equation 5 simplifies to equation 6.

$$\langle k_t \rangle = \frac{1}{4} k_t^{s,s} + \frac{1}{2} k_t^{s,l} + \frac{1}{4} k_t^{l,l} \tag{6}$$

Equal concentrations of reacting species exist when equal concentrations of RAFT agent (for the macroRAFT and initial RAFT species) are employed resulting in a simple relationship for the dependence of $k_t^{s,l}$ on the average termination rate coefficient k_t for equal size radicals (equation 7).

$$k_t^{s,l} = 2\langle k_t \rangle - \frac{1}{2} k_t^{s,s} - \frac{1}{2} k_t^{l,l} \tag{7}$$

To describe the termination rate coefficient's dependence on chain length, the geometric and harmonic means are employed (equations 8 and 9).[35]

$$k_t^{s,l} = k_{t0} (s \cdot l)^{-\varphi/2} \tag{8}$$

$$k_t^{s,l} = k_{t0} \left(\frac{2s \cdot l}{s + l} \right)^{-\varphi} \tag{9}$$

The extent that the termination rate coefficient depends on radical size for similar size macroradicals (*ss* or *ll*), i.e., macroradicals associated with the same macroRAFT distribution, is denoted α and the extent that the termination rate coefficient depends on radical size for disparate size macroradicals (*sl* and *ls*), i.e., macroradicals associated with different macroRAFT distributions, is denoted φ.

To summarize, the procedure for accessing the extent that the termination rate coefficient depends on disparate length radicals, i.e., φ, is as follows: (1) use the RAFT-CLD-T method to determine the chain length dependence for equal length radicals terminating (i.e., α); (2) obtain a prepolymerized macroRAFT species of chain length greater than one; (3) monitor the polymerization rate for the reaction mixture containing the RAFT agent, initiator, monomer and the prepolymerized macroRAFT species; (4) determine $k_t^{s,l}$ using the above methodology and α and (5) elucidate φ_{out} via constructing a double-log plot of equation 8 or 9 and obtaining a best fit to the slope.

Model Parameters

The material properties and kinetic parameters for methyl acrylate (MA), the initiator 2,2-azobisisobutyronitrile (AIBN) and the RAFT agent methoxycarbonylethyl phenyldithioacetate[32] (MCEPDA) are incorporated into the model (Table 1) including the addition, fragmentation, initiation and the initial termination rate coefficients (k_{add}, k_{frag}, k_i and k_{t0}), along with the initiator decomposition, propagation and reinitiation rate coefficients (k_d, k_p and $k_{p,rein}$) and the monomer, RAFT agent and initiator concentrations at time zero. For simplicity, the gel effect is not taken into account. All simulations were carried out using the program package PREDICI®, version 6.36.1, on an Athlon 64 X2 Dual Core Processor 3800+ IBM-compatible computer.

Results and Discussion

Accounting for fast propagation-elucidation of k_t for similar and disparate size radicals

First, the impact of fast propagation (neglecting intra-molecular chain transfer) on

Table 1.
Input parameters used for the kinetic modelling of the RAFT mediated acrylate FRP initiated with AIBN.[a)]

k_{add}[30]	k_{frag}/s^{-1}[30]	k_I[30]	k_{to}[28]
$1.4 \cdot 10^6$	$1.0 \cdot 10^5$	$1.57 \cdot 10^3$	$1.0 \cdot 10^9$
k_d/s^{-1}[28,52]	k_p[53]b	$k_{p,rein}$[28]	f[32]
$8.4 \cdot 10^{-6}$	$3.3 \cdot 10^4$	$3.3 \cdot 10^4$	0.7
$[MA]_o$[28,53]	$[MCEPDA]_o$[30]	$[AIBN]_o$[32]	$T/°C$
10.2	$3.7 \cdot 10^{-2}$	$3.0 \cdot 10^{-3}$	60

[a)] All rate coefficients are given in L mol^{-1} s^{-1} and all concentrations are given in mol L^{-1} unless otherwise indicated.

[b] Propagation rate coefficient here is for end chain propagation only.

Table 2.

φ_{out} is presented as determined from the slope of the best linear fit using the geometric mean to the simulated data for the RAFT mediated MA polymerization. Various chain lengths for the macroRAFT species, $i^{prepolymer}$, and input values for the scaling exponent for equal α and disparate φ size termination are presented.

α_{in}	φ_{in}	$i^{prepolymer}$	Slope of best linear fit	φ_{out}
0.16	0.16	32	−0.0860	0.172
0.16	0.16	56	−0.0839	0.168
0.16	0.16	82	−0.0873	0.175
0.4	0.4	32	−0.194	0.388
0.4	0.4	56	−0.160	0.320
0.4	0.4	82	−0.133	0.266
0.8	0.8	32	−0.372	0.744
0.8	0.8	56	−0.205	0.410
0.8	0.8	82	+0.165	−0.330

the method's ability to predict the termination rate coefficient's dependence on both similar and disparate size radicals is investigated. To this end, the simultaneous polymerization of two disparate length RAFT distributions is simulated.

Figure 1 shows an example of a double-log plot of equation 8 (i.e., the geometric mean) where the slope yields $-1/2\boldsymbol{\varphi}_{out}$. The value of the slope provides direct feedback as to how accurately the method predicts the chain length dependence of k_t for disparate size radicals since the input $\boldsymbol{\alpha}$ and $\boldsymbol{\varphi}$ values ($\boldsymbol{\varphi}_{in}$) are known. One obvious potential source of error lies in the use of an average (geometric or harmonic) of each distribution's average chain length; however, using RAFT chemistry the polydispersity of the distribution can be minimized. Additionally, this is currently the only proposed method able to address this complex problem of elucidation of the chain length dependence of k_t for both similar and disparate size radicals. The method predicts $\boldsymbol{\varphi}$ more accurately ($\boldsymbol{\varphi}_{in} - \boldsymbol{\varphi}_{out} = \pm 0.012$, where, for the remainder of the manuscript, the subscripts in and out are used to denote the model input parameters and model output values, respectively) when the termination rate coefficient for both equal and disparate length radicals depends less on the chain lengths, i.e., $\boldsymbol{\alpha}_{in}$ and $\boldsymbol{\varphi}_{in}$, respectively, are equal to either 0.16 or 0.4. When a higher extent of chain length dependence is taken into account (i.e., $\boldsymbol{\alpha}_{in}$ and $\boldsymbol{\varphi}_{in}$ are equal to 0.8) the method predicts $\boldsymbol{\varphi}_{out}$ with less accuracy ($\boldsymbol{\varphi}_{in} - \boldsymbol{\varphi}_{out} = 0.056$). Tables 2 and 3 reveal that the method's accuracy decreases when greater extents of chain length dependent termination are assumed. Additionally, when greater extents of chain length dependent termination are assumed,

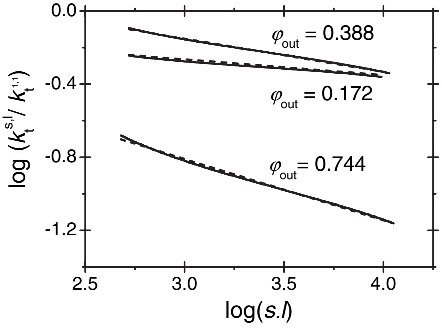

Figure 1.

A double-log plot of $k_t^{s,l}$ normalized by $k_t^{1,1}$ vs. the product of the log of each distribution's average chain length (sl) is presented for the simulated MA polymerization for α_{in} and φ_{in} are equal to 0.16, 0.4, and 0.8. The dashed line is the best linear fit; the slope of which is equal to $-1/2\varphi_{out}$. The macroRAFT species was prepolymerized to an initial average chain length equal to 32. The fit is for ~3% conversion after the macroRAFT species is administered to approximately 85% conversion, which corresponds to the range that the product of the disparate lengths increases linearly with polymerization time.

Table 3.

φ_{out} is presented as determined from the slope of the best linear fit using the harmonic mean to the simulated data for the RAFT mediated MA polymerization. Various chain lengths for the macroRAFT species, $i^{prepolymer}$, and input values for the scaling exponent for equal α and disparate φ size termination are presented.

α_{in}	φ_{in}	$i^{prepolymer}$	Slope of best linear fit	φ_{out}
0.16	0.16	32	−0.184	0.184
0.16	0.16	56	−0.176	0.176
0.16	0.16	82	−0.180	0.180
0.4	0.4	32	−0.314	0.314
0.4	0.4	56	−0.364	0.364
0.4	0.4	82	−0.300	0.300
0.8	0.8	32	−0.527	0.527
0.8	0.8	56	−0.486	0.486
0.8	0.8	82	−0.378	0.378

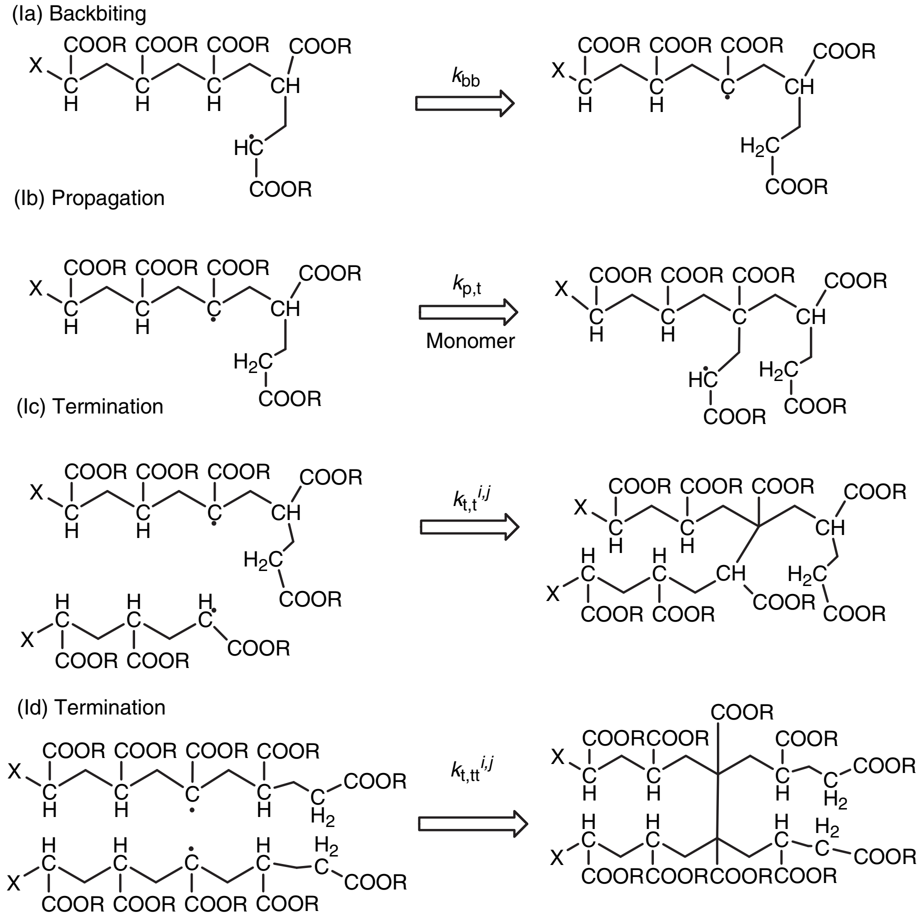

Scheme 1.
Tertiary Radical Formation (Backbiting) and Mid-Chain Radical Propagation and Termination.

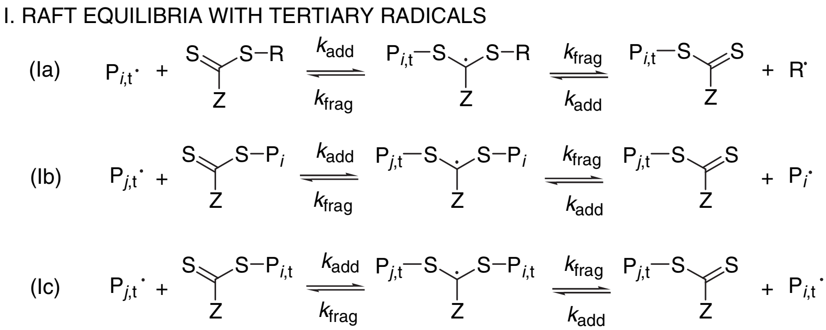

Scheme 2.
Basic Reactions for Tertiary Radical Formation (Backbiting) and Mid-Chain Radical Propagation, Termination and RAFT Equilibria.

Table 4.
Backbiting and tertiary radical formation parameters necessary for the kinetic modelling of the RAFT mediated acrylate FRP initiated with AIBN.[a)]

k_{bb}/s^{-1}[30]	$k_{p,t}$[30]	$k_{t,t}^{i,j}$[30]	$k_{t,tt}^{i,j}$[30]	$k_{add,t}$[30]	$k_{frag,t}$/s^{-1}[30]
$1.623 \cdot 10^3$	55	$1.0 \cdot 10^8$	$1.0 \cdot 10^7$	$1.4 \cdot 10^6$	$1.0 \cdot 10^5$

[a)] All rate coefficients are given in L mol^{-1} s^{-1} and all concentrations are given in mol L^{-1} unless otherwise indicated.

i.e., $\boldsymbol{\alpha}_{in}$ and $\boldsymbol{\varphi}_{in}$ are equal to either 0.4 or 0.8, the method's accuracy also decreases with increasing prepolymer chain length and the harmonic mean is observed to more accurately represents the data.

Accounting for Backbiting – Elucidation of k_t for Only Similar Size Radicals

To begin backbiting is accounted for via inclusion of the reaction steps for tertiary radical, $P_{i,t}^{\bullet}$, formation (Ia), propagation (Ib) and termination (Ic and Id) into the PREDICI® simulation (see Scheme 1). These reactions depend on the rate coefficients for backbiting, k_{bb}, tertiary radical propagation, $k_{p,t}$ and tertiary radical termination, which occurs either between two tertiary radicals, $k_{t,tt}^{i,j}$, or between a mid-chain and an end-chain radical, $k_{t,t}^{i,j}$, where the moiety X represents the continuing chain. Additionally, the model was expanded to account for the reactions for the RAFT equilibria of tertiary radicals (see Scheme 2). The pre-equilibrium of a tertiary radical with the initial RAFT agent (Ia) yields a macroRAFT species that is attached mid-chain. Additionally, the core equilibrium, where the macroRAFT species is formed from an end-chain (Ib) or a mid-chain (Ic) radical, is taken into account. The pre-equilibrium and the core equilibrium are governed by $k_{add,t}$ and $k_{frag,t}$, respectively. All necessary parameters for the kinetic modelling of intramolecular chain transfer are given in Table 4. There are no kinetic parameters to date for how backbiting occurs during the RAFT mediated AIBN initiated methyl acrylate polymerization, thus the kinetic parameters for the RAFT mediated AIBN initiated dodecyl acrylate FRP were used.

Accounting for mid-chain radical formation has been shown to lead to virtual monomer reaction orders (i.e., ω) greater than one.[44] Equation 10 depicts the

Table 5.
ω and α_{out} are presented for various backbiting and termination rate coefficients and α_{in} values as predicted via simulation of the RAFT mediated MA polymerization. α_{out} is determined from the slope of a double-log plot of equation 8 including data from 10 to 40 % conversion. The impact of different α^{t}, α^{tt}, $k_{t,t}$ and $k_{t,tt}$ values on α_{out} is shown.[a)]

k_{bb}/s^{-1}[31]	$k_{t,t}$	$k_{t,tt}$	α^{t}	α^{tt}	α_{in}/α_{out}	ω
0	0	0	0	0	0.4/0.39	1.0
$1.623 \cdot 10^3$	$1.0 \cdot 10^9$	$1.0 \cdot 10^9$	0	0	0.0/0.01	2.5
$1.623 \cdot 10^3$	$1.0 \cdot 10^9$	$1.0 \cdot 10^9$	0	0	0.4/0.40	4.3
$1.623 \cdot 10^3$	$1.0 \cdot 10^8$	$1.0 \cdot 10^7$	0	0	0.4/0.40	2.2
$1.623 \cdot 10^3$	$1.0 \cdot 10^9$	$1.0 \cdot 10^9$	0	0	0.16/0.16	3.2
$1.623 \cdot 10^3$	$1.0 \cdot 10^8$	$1.0 \cdot 10^7$	0	0	0.16/0.16	1.6
$1.623 \cdot 10^3$	$1.0 \cdot 10^9$	$1.0 \cdot 10^9$	0.4	0	0.4/0.40	3.3
$1.623 \cdot 10^3$	$1.0 \cdot 10^8$	$1.0 \cdot 10^7$	0.4	0	0.4/0.41	1.3
$1.623 \cdot 10^3$	$1.0 \cdot 10^9$	$1.0 \cdot 10^9$	0.4	0.4	0.4/0.37	2.6
$1.623 \cdot 10^3$	$1.0 \cdot 10^8$	$1.0 \cdot 10^7$	0.4	0.4	0.4/0.41	1.3

[a)] All rate coefficients are given in L mol^{-1} s^{-1} and all concentrations are given in mol L^{-1} unless otherwise indicated.

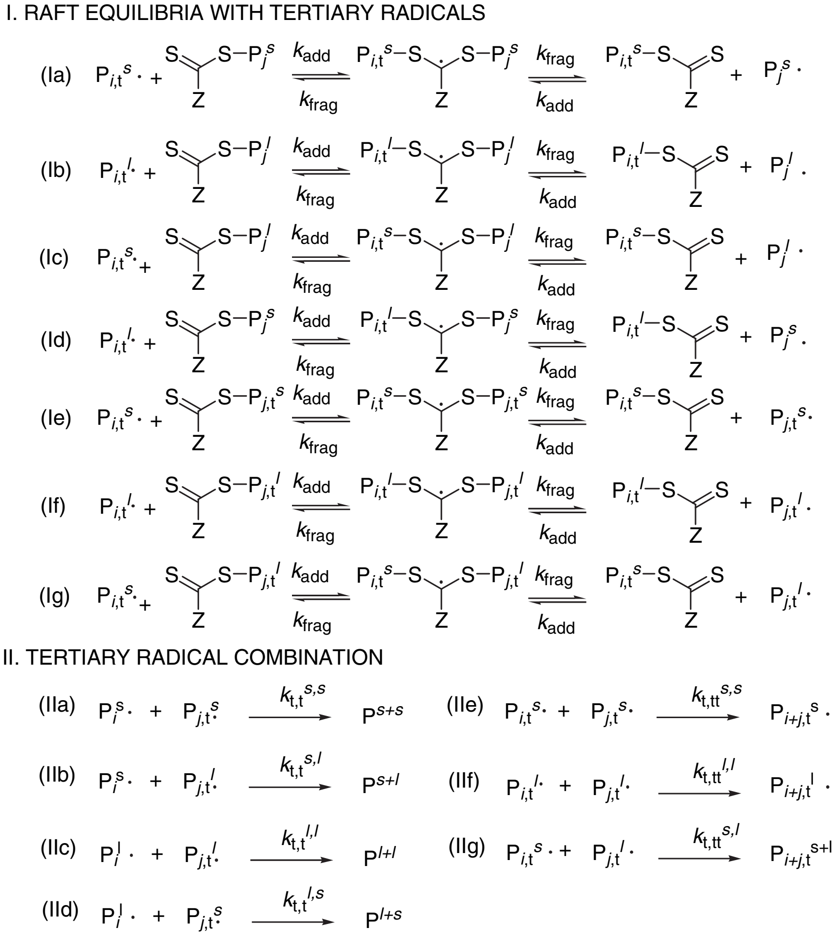

Scheme 3.
The Core Equilibrium and Termination Reactions for Two Simultaneous RAFT FRPs when Mid-Chain Radical Formation and Subsequent Reactions are Taken into Account.

important components from the classical polymerization rate equation that are necessary to evaluate the relationship between the polymerization rate, the initiator and monomer concentrations and the termination rate coefficient when the assumption of a steady state radical concentration is made.

$$R_{\mathrm{p}} \approx [\mathrm{M}]^{\omega}\left(\frac{[\mathrm{I}]}{k_{\mathrm{t}}^{\mathrm{i,i}}}\right)^{0.5} \tag{10}$$

Taking the logarithmic form of equation 10 and accounting for the chain length dependence of k_{t} results in an equation for determination of ω:

$$\begin{aligned}\log(R_{\mathrm{p}}) - \log([\mathrm{I}]^{1/2}) - \log(i^{\alpha/2}) \\ = \omega \log([\mathrm{M}])\end{aligned} \tag{11}$$

The impact of the value and chain length dependence of the k_{t}s that are introduced when backbiting and mid-chain radicals are accounted for (i.e., $k_{\mathrm{t,t}}^{i,j}$, $k_{\mathrm{t,tt}}^{i,j}$, α^{t} and α^{tt}) on the virtual monomer reaction order (ω) was investigated for the case that takes into account only similar size radicals. Table 5 shows that a greater than classical mono-

Table 6.
φ_{out} is presented as determined from the slope of the best linear fit using the geometric mean to the simulated data for the RAFT mediated MA polymerization. Various chain lengths for the macroRAFT species, $i^{prepolymer}$, and input values for the scaling exponent for equal α and disparate φ size termination are presented. All termination events involving mid-chain radicals are assumed chain length independent (i.e., α^{t} and $\alpha^{tt} = 0$).

α_{in}	φ_{in}	$i^{prepolymer}$	ω	Slope of best linear fit	φ_{out}
0.16	0.16	32	1.2	−0.0835	0.167
0.16	0.16	56	1.2	−0.0807	0.161
0.16	0.16	82	1.2	−0.0793	0.159
0.4	0.4	32	1.5	−0.200	0.400
0.4	0.4	56	1.5	−0.201	0.402
0.4	0.4	82	1.5	−0.195	0.390
0.8	0.8	32	2.5	−0.419	0.838
0.8	0.8	56	2.5	−0.429	0.858
0.8	0.8	82	2.5	−0.451	0.902

mer reaction order ($\omega = 1$, classically) is predicted when intramolecular chain transfer is important. Additionally, ω decreases both when mid-chain radical termination is slower than end-chain radical termination (i.e., $k_{t,tt}^{i,j} < k_{t,t}^{i,j} < k_{t}^{i,j}$) and when mid-chain radical termination is chain length dependent (i.e., α^{t} and α^{tt} are greater than zero). Additionally, increasing α_{in} (i.e., from 0.16 to 0.4) increases the polymerization rate's dependence on the monomer concentration (ω). Most importantly, Table 5 clearly shows that when the data is carefully analyzed (i.e., the virtual monomer reaction order is ascertained) that the method predicts accurately the extent that the termination rate coefficient depends on the radical's chain length when backbiting is accounted for. Thus, elucidation of the virtual monomer reaction order eliminates the need to ascertain the adjustable *backbiting* kinetic parameters.

Accounting for Backbiting - Elucidation of k_t for Disparate Size Radicals

Accessing the chain length dependence of the termination rate coefficient for *disparate* length radicals is a process that is significantly more complex when intramolecular chain transfer occurs. For example, two new termination rate coefficients ($k_{t,t}^{i,j}$ and $k_{t,tt}^{i,j}$) are accounted for that may differ in value and chain length dependence from conventional $k_{t}^{i,j}$. To investigate the impact of backbiting and tertiary radicals on the method's ability to predict the chain length dependence of k_t for disparate length radicals, i.e., φ, where $k_{t}^{s,l} \propto (sl)^{-\varphi/2}$, the method

Table 7.
φ_{out} is presented as determined from the slope of the best linear fit using the harmonic mean to the simulated data for the RAFT mediated MA polymerization. Various chain lengths for the macroRAFT species, $i^{prepolymer}$, and input values for the scaling exponent for equal α and disparate φ size termination are presented. All termination events involving mid-chain radicals are assumed chain length independent (i.e., α^{t} and $\alpha^{tt} = 0$).

α_{in}	φ_{in}	$i^{prepolymer}$	ω	Slope of best linear fit	φ_{out}
0.16	0.16	32	1.2	−0.159	0.159
0.16	0.16	56	1.2	−0.150	0.150
0.16	0.16	82	1.2	−0.144	0.144
0.4	0.4	32	1.5	−0.397	0.397
0.4	0.4	56	1.5	−0.362	0.362
0.4	0.4	82	1.5	−0.352	0.352
0.8	0.8	32	2.5	−0.800	0.800
0.8	0.8	56	2.5	−0.784	0.784
0.8	0.8	82	2.5	−0.782	0.782

was expanded to include the necessary reactions for accounting for the core equilibrium and termination events when two RAFT distributions polymerize simultaneously (see Scheme 3). Elucidation of φ_{out} when backbiting is important, first requires determination of the virtual monomer reaction order for the specific polymerization condition.

Tables 6 and 7 present ω as a function of termination and show that ω increases with increasing chain length dependent termination, i.e., ω is equal to 1.2, 1.5 and 2.5 when α_{in} and φ_{in} are equal to 0.16, 0.4 and 0.8, respectively. Additionally, when backbiting and virtual monomer reaction orders greater than one are accounted for, the method predicts φ_{out} better than the method that considers only fast propagation (see Tables 2 and 3).

Since the assumption that equal concentrations of reacting species is guaranteed via employing equal concentrations of RAFT agents (and neglecting a potential CLD of the RAFT equilibrium reactions) the only other assumption that could cause the model to inaccurately predict φ_{out} is the assumption that each RAFT distribution is represented adequately by its average chain length. In fact, when backbiting is neglected and fast propagation is accounted for, the model predicts a more polydisperse "short" macroRAFT distribution that increases in polydispersity when the termination rate decreases more rapidly (i.e., with increasing chain length dependence, the geometric mean and greater radical size disparity (s-l)). When backbiting is accounted for a more monodisperse "short" macroRAFT distribution is predicted and consequently the method predicts more accurately φ_{out}. In this context, it is important to note that the macroRAFT distributions' polydispersity can be controlled via changing the initiation conditions. Thus, when the data is analyzed with extreme care and the reaction thoroughly characterized (i.e., intramolecular chain transfer is accounted for and ω is determined), determining the extent that the termination rate coefficient depends on disparate size radicals for the acrylate polymerization may be possible using this methodology.

Conclusions

RAFT chemistry is used to elucidate the extent that $k_{\text{t}}^{s,l}$ depends on disparate length radicals for the fast propagating acrylate free radical polymerization, i.e., φ. The method builds upon a previously developed method that is able to access $k_{\text{t}}^{s,l}$ for the model monomer system styrene. Application of the method to the methyl acrylate polymerization shows the importance of considering intramolecular chain transfer (backbiting and the subsequent mid-chain radical reactions including RAFT equilibria). Accounting for intramolecular chain transfer reveals that the method's predictive capability is sensitive to the polymerization rate's dependence on monomer concentration, i.e., the virtual monomer reaction order. Simulation is used to illustrate that the virtual monomer reaction order depends on the polymerization conditions such as the termination rate coefficient's value and chain length dependence. Most significantly, knowledge of the virtual monomer reaction order may indeed allow for the accurate determination of the extent that k_{t} depends on radical size (both α and φ) for the acrylate FRP. Since the method appears to be robust enough to handle acrylate polymerizations, it is our recommendation that the method be validated experimentally; yet (based on this work) it appears that experimental validation should be carried out initially using a slowly propagating monomer such as styrene to avoid the more complex data analysis necessary for some of the more reactive monomers.

Acknowledgements: We thank the Australian Research Council (ARC) for their financial support in the form of a Discovery Grant to C.B.-K. and M.H.S., an Australian Professorial Fellowship to C.B.-K. as well as a Federation

Fellowship to T.P.D. Additionally, we recognize Dr. Leonie Barner and Mr. Istvan Jacenyik for their outstanding management of CAMD.

[1] C. Decker, *Eur. Polym. J.* **2005**, *7–8*, 30–32.

[2] A. N. F. Peck, R. A. Hutchinson, *Macromolecules* **2004**, *37*, 5944–5951.

[3] H. Lu, J. A. Carioscia, J. W. Stansbury, C. N. Bowman, *Dent. Mat.* **2005**, *21*, 1129–1136.

[4] J. Ge, M. Trujillo, J. W. Stansbury, *Dental Materials* **2005**, *21*, 1163–1169.

[5] J. Chiefari, Y. K. Chong, F. Ercole, J. Krstina, J. Jeffery, T. P. T. Le, R. T. A. Mayadunne, G. F. Meijs, C. L. Moad, G. Moad, E. Rizzardo, S. H. Thang, *Macromolecules* **1998**, *31*, 5559–5562.

[6] T. Otsu, *Journal of Polymer Science Part A: Polymer Chemistry* **2000**, *38*, 2121–2136.

[7] C. Barner-Kowollik, T. P. Davis, J. P. A. Heuts, M. H. Stenzel, P. Vana, M. Whittaker, *J. Polym. Sci. Part A: Polym. Chem.* **2003**, *41*, 365–375.

[8] G. Chen, D. Huynh, P. L. Felgner, Z. Guan, *J. Am. Chem. Soc.* **2006**, *128*, 4298–4302.

[9] R. T. A. Mayadunne, E. Rizzardo, J. Chiefari, J. Kristina, G. Moad, A. Postma, S. H. Thang, *Macromolecules* **2000**, *33*, 243–245.

[10] C. J. Hawker, A. W. Bosman, E. Harth, *Chem. Rev.* **2001**, *101*, 3661–3688.

[11] Y. K. Chong, T. P. T. Le, G. Moad, E. Rizzardo, S. H. Thang, *Macromolecules* **1999**, *32*, 2071–2074.

[12] M. L. Becker, J. Liu, K. L. Wooley, *Biomacromolecules* **2005**, *6*, 220–228.

[13] H. Gao, K. Matyjaszewski, *Macromolecules* **2006**, *39*, 4960–4965.

[14] P. E. M. Allen, C. R. Patrick, *Makromol. Chem.* **1961**, *47*, 154–167.

[15] M. Buback, A. Kuelpmann, C. Kurz, *Macromol. Chem. Phys.* **2002**, *203*, 1065–1070.

[16] P. G. de Gennes, *J. Chem. Phys.* **1982**, *76*, 3316–3321.

[17] G. I. Litvinenko, V. A. Kaminsky, *Prog. React. Kinetics* **1994**, *19*, 139–193, and references within.

[18] G. T. Russell, *Macromol. Theory Simul.* **1995**, *4*, 497–517.

[19] G. Johnston-Hall, A. Theis, M. J. Monteiro, T. P. Davis, M. H. Stenzel, C. Barner-Kowollik, *Macromol. Chem. Phys.* **2005**, *206*, 2047–2053.

[20] M. Buback, M. Busch, C. Kowollik, *Macromol. Theory Simul.* **2000**, *9*, 442–452.

[21] M. Buback, M. Egorov, R. G. Gilbert, V. A. Kaminsky, O. F. Olaj, F. Oskar, G. T. Russell, *Macromol. Chem. Phys.* **2002**, *203*, 2570–2582.

[22] M. Buback, R. G. Gilbert, G. T. Russell, D. J. T. Hill, G. Moad, K. F. O'Driscoll, J. Shen, M. A. Winnik, *J. Polym. Sci. Part A: Polym. Chem.* **1992**, *30*, 851–863.

[23] M. Buback, E. Mueller, G. T. Russell, *J. Phys. Chem. A* **2006**, *110*, 3222–3230.

[24] G. B. Smith, J. Heuts, G. T. Russell, *Macromol. Symp.* **2005**, *226*, 133–146.

[25] P. Vana, T. P. Davis, C. Barner-Kowollik, *Macromol. Rapid. Commun.* **2002**, *23*, 952–956, and references within.

[26] M. Buback, F. D. Kuchta, *Macromol. Chem. Phys.* **1997**, *198*, 1455–1480.

[27] A. Feldermann, M. H. Stenzel, T. P. Davis, P. Vana, C. Barner-Kowollik, *Macromolecules* **2004**, *37*, 2404–2410.

[28] A. Theis, A. Feldermann, N. Charton, M. H. Stenzel, T. P. Davis, C. Barner-Kowollik, *Macromolecules* **2005**, *38*, 2595–2605.

[29] T. Junkers, A. Theis, M. Buback, T. P. Davis, M. H. Stenzel, P. Vana, C. Barner-Kowollik, *Macromolecules* **2005**, *38*, 9497–9508.

[30] A. Theis, A. Feldermann, N. Charton, T. P. Davis, M. H. Stenzel, C. Barner-Kowollik, *Polymer* **2005**, *46*, 6797–6809.

[31] G. Johnston-Hall, A. Theis, M. J. Monteiro, T. P. Davis, M. H. Stenzel, C. Barner-Kowollik, *Macromol. Chem. Phys.* **2005**, *206*, 2047–2053.

[32] A. Theis, T. P. Davis, M. H. Stenzel, C. Barner-Kowollik, *Macromolecules* **2005**, *38*, 10323–10327.

[33] A. Theis, T. P. Davis, M. H. Stenzel, C. Barner-Kowollik, *Polymer* **2006**, *47*, 999–1010.

[34] M. Buback, T. Junkers, P. Vana, *Macromol. Rapid. Comm.* **2005**, *26*, 796–802.

[35] T. M. Lovestead, A. Theis, T. P. Davis, M. H. Stenzel, C. Barner-Kowollik, *Macromolecules* **2006**, *39*, 4975–4982.

[36] A. Theis, M. H. Stenzel, T. P. Davis, C. Barner-Kowollik, "Obtaining Chain Length Dependent Termination Rate Coefficients via Thermally Initiated RAFT Experiments: Current Status and Future Challanges," in *ACS Symposium Series on Living/Controlled Free Radical Polymerization*, K. Matyjaszewski, Ed. ACS Press: Washington, D.C., **2006**; *944*, 486–500.

[37] M. Buback, M. Egorov, A. Feldermann, *Macromolecules* **2004**, *37*, 1768–1776.

[38] S. Perrier, C. Barner-Kowollik, J. F. Quinn, P. Vana, T. P. Davis, *Macromolecules* **2002**, *35*, 8300–9306.

[39] J. B. McLeary, J. M. McKenzie, M. P. Tonge, R. D. Sanderson, B. Klumperman, *Chem. Commun.* **2004**, 1950–1951.

[40] S. Beuermann, J. Paquet, D.A., J. H. McMinn, R. A. Hutchinson, *Macromolecules* **1996**, *29*, 4206–4215.

[41] K. Tanaka, B. Yamada, C. M. Fellows, R. G. Gilbert, T. P. Davis, L. H. Yee, G. B. Smith, M. T. L. Rees, G. T. Russell, *J. Poly. Sci. Part A: Poly. Chem.* **2001**, *39*, 3902 + 3915.

[42] J. M. Asua, S. Beuermann, M. Buback, P. Castignolles, B. Charleux, R. G. Gilbert, *Macromol. Chem. Phys.* **2004**, *205*, 2151–2160.

[43] M. Busch, M. Muller, *Macromol Symp* **2004**, *206*, 399–418.

[44] A. N. Nikitin, R. A. Hutchinson, *Macromolecules* **2005**, *38*, 1581–1590.

[45] E. Chernikova, A. Morozov, E. Leonova, E. Garina, V. Golubev, C. Bui, B. Charleux, *Macromolecules* **2004**, *37*, 6329–6339.

[46] C. Quan, M. Soroush, M. C. Grady, J. E. Hansen, W. J. Simonsick, Jr., *Macromolecules* **2005**, *38*, 7619–7628.

[47] A. Postma, T. P. Davis, G. Li, G. Moad, M. S. O'Shea, *Macromolecules* **2006**, In Press.

[48] E. Sato, T. Emoto, P. B. Zetterlund, B. Yamada, *Macromolecular Chemistry and Physics* **2004**, *205*, 1829–1839.

[49] A. N. Nikitin, P. Castignolles, B. Charleux, J.-P. Vairon, *Macromolecular Rapid Communications* **2003**, *24*, 778–782.

[50] C. Barner-Kowollik, J. F. Quinn, T. L. U. Nguyen, J. P. A. Heuts, T. P. Davis, *Macromolecules* **2001**, *34*, 7849–7857.

[51] M. Wulkow, M. Busch, T. P. Davis, C. Barner-Kowollik, *J. Polym. Sci. Part A: Polym. Chem.* **2004**, *42*, 1441–1448.

[52] N. Charton, A. Feldermann, A. Theis, M. H. Stenzel, T. P. Davis, C. Barner-Kowollik, *J. Polym. Sci. Part A: Polym. Chem.* **2004**, *42*, 5170–5179.

[53] M. Buback, C. H. Kurz, C. Schmaltz, *Macromol. Chem. Phys.* **1998**, *199*, 1721–1727.